

# Tetravariate Point-Process Model for the Continuous Characterization of Cardiovascular-Respiratory Dynamics during Passive Postural Changes

Michele Orini<sup>1</sup>, Gaetano Valenza<sup>2,3</sup>, Luca Citi<sup>2</sup>, Riccardo Barbieri<sup>2</sup>

<sup>1</sup>GTC, I3A, University of Zaragoza, and CIBER-BBN, Spain

<sup>2</sup>Neuroscience Statistics Research Laboratory, Harvard Medical School, Massachusetts General Hospital, Boston, MA, USA, and Massachusetts Institute of Technology, Cambridge, MA, USA

<sup>3</sup>Interdepartmental Research Center "E Piaggio", University of Pisa, Italy

## Abstract

*In this study, we present a new methodology for time-varying characterization of cardiovascular (CV) control, which includes RR interval (RRI), systolic arterial pressure (SAP), respiration (RSP) and pulse transit time (PTT). Within a multivariate model, CV dynamics are represented as stochastic point processes whose means has a tetravariate autoregressive structure. Such framework provides the simultaneous time-frequency assessment of: (i) both arms of the SAP-RRI loop, along baroreflex and mechanical feedforward pathways; (ii) Respiratory sinus arrhythmia (RSA), through the direct evaluation of the interactions between RSP and the RRI; (iii) the coupling between cardio-respiratory activity and vascular tone through quantification of the interactions between PTT and the other CV variables. We validated the model by characterizing CV control in 16 healthy subjects during a tilt table test, and we were able to confirm a satisfactory model's goodness-of-fit. We further estimated transfer function gains, instantaneous powers and directed coherences, and observed that RSP strongly drove respiratory-related oscillations in all the other CV variables, and that PTT depended on RRI dynamics rather than blood pressure variations. During head-up tilt, baroreflex sensitivity and RSA decreased, while the gain from RRI to SAP increased, thus confirming previous physiological characterizations.*

## 1. Introduction

The assessment of cardiovascular (CV) control, both in health and disease, is of primary importance to improve our understanding and early detection of CV dysfunctions. For a comprehensive characterization of CV functioning, a multivariate non-stationary framework is needed. In this study, we propose a multivariate point-process model to study the CV system, which takes into account the automatic control of the circulation. The model includes four

CV variables, namely, the RR interval (RRI), systolic arterial pressure (SAP), respiration (RSP) and pulse transit time (PTT). With respect to previous multivariate models [1–3], in this framework we directly considered the influence of respiration, through the input RSP, and of vascular dynamics, through the inclusion of PTT, which is strictly related to pulse wave velocity and arterial stiffness [4]. Additionally, the multivariate point process approach allows to give model's goodness-of-fit measures, and offers the possibility of estimating time-varying indices of causal coupling [5] for the respiratory and low frequency (LF) spectral bands separately. We used this model to characterize changes in the dynamic interactions between all four CV variables during a tilt table test.

## 2. Methodology

### 2.1. The tetravariate point-process model

Let's define as  $t_n^R$  and  $t_n^P$  the time occurrence of the  $n$ -th R wave in the ECG and the arrival time of the systolic pressure peak to the finger, respectively (see Fig. 1); be  $w_n^{RRI} = t_{n+1}^R - t_n^R$  and  $w_n^{PTT} = t_n^P - t_n^R$  the  $n$ -th RRI and PTT, respectively. Be  $x_n^{RSP} = x^{RSP}(t_n^R)$  and  $x_n^{SAP} = x^{SAP}(t_n^P)$ , the respiratory signal sampled at heart beat occurrence and the systolic pressure value estimated at the finger, respectively (see Fig. 1).

The probability density function of RRI and PTT can be described for any  $t > t_n^R$  by an inverse Gaussian (IG) distribution [6]:

$$f_J^{IG}(t) = \sqrt{\frac{\lambda_J(t)}{2\pi[t - t_n^R]^3}} \exp\left(-\frac{\lambda_J(t)[t - t_n^R - \mu_J(t)]^2}{2\mu_J^2(t)[t - t_n^R]}\right) \quad (1)$$

where  $J \in \{\text{RRI}, \text{PTT}\}$ , and  $\mu_J(t)$  and  $\lambda_J(t)$  are the mean and the shape parameters. Note that when (1) is used to describe the statistical structure of PTT,  $f_J^{IG}(t)$  is well defined for  $t_n^R \leq t \leq t_n^P$ . Whithin this framework, the variance of

PTT and RRI can be estimated as  $\sigma_J^2 = \mu_J^3(t)/\lambda_J(t)$  [6]. The probability density function of SAP and RSP is described by a Normal distribution:

$$f_J^N(t) = \sqrt{\frac{1}{2\pi\sigma_J^2(t)}} \exp\left(-\frac{[x_n^J - \mu_J(t)]^2}{2\sigma_J^2(t)}\right) \quad (2)$$

where  $J \in \{\text{SAP}, \text{RSP}\}$  (see Fig. 1). In this case, the choice of a normal distribution, rather than an IG, is motivated by the fact that these variables do not represent the inter-event-interval of a point process but rather measurements of signals for which an additive Gaussian noise model can be assumed.

The considered CV variables are continuously interacting, so that at any time the value of one variable depends on its recent history as well as on the recent history of any other variable. This dependence is embedded in the point-process framework by assuming a multivariate autoregressive structure for any  $\mu_J(t)$ :

$$\underline{M}(t) = \underline{A}_0(t) + \sum_{k=1}^Q \underline{A}_k(t) \underline{W}_{n-k} \quad (3)$$

where  $\underline{M}(t) = [\mu_{\text{RRI}}(t), \mu_{\text{PTT}}(t), \mu_{\text{SAP}}(t), \mu_{\text{RSP}}(t)]^T$  is the vector of the means of distributions (1)-(2),  $\underline{A}_{k,ij}(t) = [a_k^{(ij)}(t)]$  is the  $4 \times 4$  matrix of the time-varying model coefficients, and  $\underline{W}_n = [w_n^{\text{RRI}}, w_n^{\text{PTT}}, x_n^{\text{SAP}}, x_n^{\text{RSP}}]^T$  is the vector of the observed regressors. Importantly, coefficients  $a_k^{(ij)}(t)$  provide a time-varying quantification of the interaction along  $j \rightarrow i$ . For example,  $a_2^{(13)}(t)$  quantifies the linear contribution that  $x_{n-2}^{\text{SAP}}$ , i.e. SAP value at  $t_{n-2}^p$ , has on  $\mu_{\text{RRI}}(t)$ , with  $t_n^R < t < t_{n+1}^R$ . Thus,  $a_k^{(31)}(t)$ ,  $a_k^{(13)}(t)$  and  $a_k^{(14)}(t)$  correspond to pathways that can be associated to the mechanical feedforward influence of RRI on SAP, baroreflex feedback from SAP to RRI, and respiratory sinus arrhythmia (RSA), respectively.

The order of the model was empirically set at  $Q = 5$ , while the temporal resolution was 0.001 s. Time-varying model coefficients are identified by Newton-Raphson maximization of the local likelihood, which also includes right censoring, and using a weighting function  $W(t - t_n^R) = 0.98^{(t-t_n^R)}$ , with  $t - t_n^R \leq 120$  s [6].

To assess the capability of the model to describe the statistical properties of the multivariate point processes, i.e. RRI and PTT, the model's goodness-of-fit is quantified. Goodness-of-fit is evaluated by representing the Kolmogorov-Smirnov (KS) plot which measures the largest distance between the cumulative distribution function of RRI and PTT series transformed to the interval (0,1] by using the time rescaling theorem [6], and the cumulative distribution function of a uniform distribution on (0,1]. The smaller the KS distances, the closer is the agreement between original RRI and PTT series and the proposed model. If the model completely captures the statistical properties of RRI and PTT, the transformed series

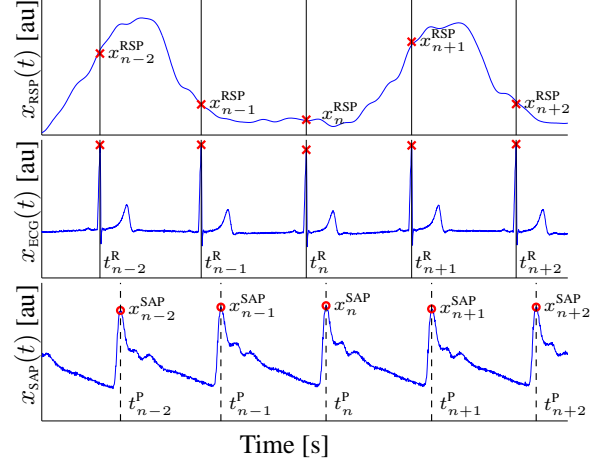


Figure 1. An example of RSP, ECG and SAP signals. Circles and crosses mark the occurrence time of a R wave,  $t_n^R$ , and arrival time of pulse wave at the finger,  $t_n^P$ , used as reference to estimate the PTT.

should be uncorrelated [6]. To quantify the degree of correlation in the rescaled series, two indices were estimated: the number of the lag points for which the correlation was outside the confidence interval,  $c_{\#}$ , and the ratio between the highest correlation and the confidence level,  $c_R$ .

## 2.2. Time-frequency CV assessment

The non-stationary transfer function of the system,  $\underline{H}(t, f) = [H_{ij}(t, f)]$ , is estimated as:

$$\underline{H}(t, f) = \left[ \underline{I} - \sum_{k=1}^Q \underline{A}_k(t) e^{-i2\pi f k} \right]^{-1} \quad (4)$$

where  $\underline{I}$  is the identity matrix. Time-frequency spectra,  $S_{ij}(t, f)$ , and directed coherence,  $\gamma_{ij}^{\text{DC}}(t, f)$ , are defined for  $\{i, j\} \in \{1, \dots, 4\}$ , as [2, 5]:

$$S_{ij}(t, f) = \sum_{m=1}^4 H_{im}(t, f) \sigma_m^2(t) H_{jm}^*(t, f) \quad (5)$$

$$\gamma_{ij}^{\text{DC}}(t, f) = \frac{\sigma_j(t) H_{ij}(t, f)}{\sqrt{\sum_{m=1}^4 \sigma_m^2(t) |H_{im}(t, f)|^2}} \quad (6)$$

Directed coherence  $\gamma_{ij}^{\text{DC}}(t, f)$  represents the ratio between the part of  $S_{ii}(t, f)$  due to process  $j$  and  $S_{ii}(t, f)$  [5]. By definition,  $\sum_{m=1}^4 |\gamma_{im}^{\text{DC}}(t, f)|^2 = 1$ .

## 2.3. Estimation of the indices of interaction

To estimate the time course of the indices of interaction, two TV spectral bands are localized in the time-frequency domain. The first one, related to respiratory activity, is defined as:  $\Omega_{\text{RSP}} = \{(t, f) | f \in [f_{\text{RSP}}(t) \pm \Delta_F]\}$ , where

$f_{\text{RSP}}(t)$  is the respiratory rate, estimated from  $S_{44}(t, f)$ , and  $\Delta_F = 0.05$  Hz. The second spectral band, related to LF spectral range, is defined as  $\Omega_{\text{LF}} = \{(t, f) | f \in [0.04, \min(0.15, f_{\text{RSP}}(t) - \Delta_F)]\}$ . Note that  $\Omega_{\text{RSP}}$  and  $\Omega_{\text{LF}}$  cannot overlap, and when  $f_{\text{RSP}}(t)$  is low,  $\Omega_{\text{RSP}}$  can include portions of the traditional LF band. If for a given  $t_0$ , the width of  $\Omega_{\text{LF}}$  is lower than  $\Delta_F$ , then  $\Omega_{\text{LF}|t=t_0} = \emptyset$ .

$\gamma_{ij,B}^{\text{DC}}(t)$  is estimated as the global maximum inside each spectral band  $\Omega_B$ , while transfer function gains,  $|H_{ij,B}(t)|$ , and instantaneous powers,  $P_{ii,B}(t)$ , are estimated by averaging  $|H_{ij}(t, f)|$  and  $S_{ii}(t, f)$  inside  $\Omega_B$ , with  $B \in \{\text{LF}, \text{RSP}\}$ .

### 3. Experimental setting

Sixteen volunteers ( $28.6 \pm 2.9$  years, 10 males) without any previous cardiovascular history underwent a head up tilt table test according to the following protocol: 4 min in early supine position ( $T_{\text{ES}}$ ), 5 min tilted head up to an angle of 70 degrees ( $T_{\text{HT}}$ ) and 4 min back to later supine position ( $T_{\text{LS}}$ ) [7, 8]. The pressure signal was recorded at the finger by the Finometer system with a sampling frequency ( $f_s$ ) of 250 Hz and without correction for the hydrostatic gradient change during tilt, whereas standard lead V4 ECG signal was recorded with  $f_s = 1$  KHz. Time occurrence of each R wave in the ECG,  $t_n^{\text{R}}$ , and systolic peaks in the pressure signal,  $\{t_n^{\text{P}}, x_n^{\text{SAP}}\}$ , were automatically determined and manually revised. The respiratory signal was recorded through a strain gauge transducer, with  $f_s = 125$  Hz.

### 4. Results

Table 1 reports the mean and standard deviation of the KS distance,  $c_{\#}$ ,  $c_{\text{R}}$  estimated for all subjects, and shows that the model was able to capture the statistical properties of the CV variables.

The median time courses, estimated across subjects, of the indices characterizing the most relevant CV interactions are shown in Fig. 2. Upper, middle and lower graphics refer to  $\gamma_{B,ij}^{\text{DC}}(t)$ ,  $|H_{B,ij}(t)|$  and  $P_{B,ii}(t)$ , respectively, while the first and the last three columns report indices estimated in  $\Omega_{\text{LF}}$  and  $\Omega_{\text{RSP}}$ , respectively. Note that the indices of those subjects for which a given index was not estimated for more than 75% of the duration of the experiment (when  $\Omega_{\text{LF}}$  is too narrow or when there is not a maximum inside the spectral band) were not included in the calculations.

To assess whether the changes in the indices were statistically significant, temporal median values were estimated in  $T_{\text{ES}}$ ,  $T_{\text{HT}}$  and  $T_{\text{LS}}$  and compared by signed rank test. To exclude fast changes during transients, the first and last 30 s of each interval were not considered in the statistical analysis, and significance was assumed for  $P < 0.05$ .

In  $\Omega_{\text{LF}}$ , PTT depended on RRI dynamics rather than blood pressure variations (Fig. 2(a),(c)); The mutual influence

Table 1. Goodness of fit as mean  $\pm$  standard deviation of KS distances,  $c_{\#}$  and  $c_{\text{R}}$ .

Signal	Model's goodness-of-fit		
	KS-dist	$c_{\#}$	$c_{\text{R}}$
PTT	$0.087 \pm 0.028$	$1.375 \pm 1.258$	$1.189 \pm 0.254$
RRI	$0.051 \pm 0.022$	$1.313 \pm 1.352$	$1.215 \pm 0.355$

of SAP and RRI was high, and during tilt directed coherence from RRI to SAP decreased (Fig. 2(b)). During tilt,  $|H_{21}(t)|$  and  $|H_{31}(t)|$ , representing RRI $\rightarrow$ PTT and RRI $\rightarrow$ SAP interactions, increased, while  $|H_{13}(t)|$ , representing baroreflex pathway, decreased. Interestingly, the decrease in  $|H_{13}(t)|$  is faster and happens earlier than the increase in  $|H_{21}(t)|$  and  $|H_{31}(t)|$  (Fig. 2(g)-(h)). This may be explained by a slower response of the mechanical feedforward pathway with respect to the faster neurally-mediated feedback baroreflex. During tilt, LF power of PTT and SAP increased (Fig. 2(o)-(q)). In  $\Omega_{\text{RSP}}$ , RSP had great influence on RRI, PTT and SAP, while, as expected, these three variables had virtual no influence on RSP (Fig. 2(d)-(f)). A decrease in RSA,  $|H_{14}(t)|$ , suggests that parasympathetic activity is reduced during tilt. Note that by construction the increase in RSA is independent from the increase in respiratory power observed during tilt.

### 5. Discussion and conclusions

In this study, we presented an innovative point-process model for the time-varying characterization of CV regulation. The model provides the simultaneous assessment of: (i) both arms of the SAP-RRI loop, along baroreflex and mechanical feedforward pathways; (ii) RSA, through the direct evaluation of the interactions between the respiratory input and the RRI; (iii) the coupling between cardio-respiratory activity and the vasculature, which is possible thanks to the quantification of the interactions between PTT and the other variables. In addition, since the CV variables are embedded in a point process framework, model coefficients and parameters are estimated in continuous time, respecting the physiological order of discrete-time events such as systole and pulse arrival time. Importantly, this framework offers the possibility of quantifying the model's goodness-of-fit [6]. The assumption of a tetravariate autoregressive structure for the model allows to analyze the causal interactions between the CV variables in the time-frequency domain [2, 5]. Results confirm that respiration can be considered as a critical external input which drives respiratory-related oscillations in other CV variables [9]. Head-up tilt provoked a decrease in the baroreflex sensitivity and in RSA, and a simultaneous increase in the gain of the feedforward mechanical effect. Also of relevance,

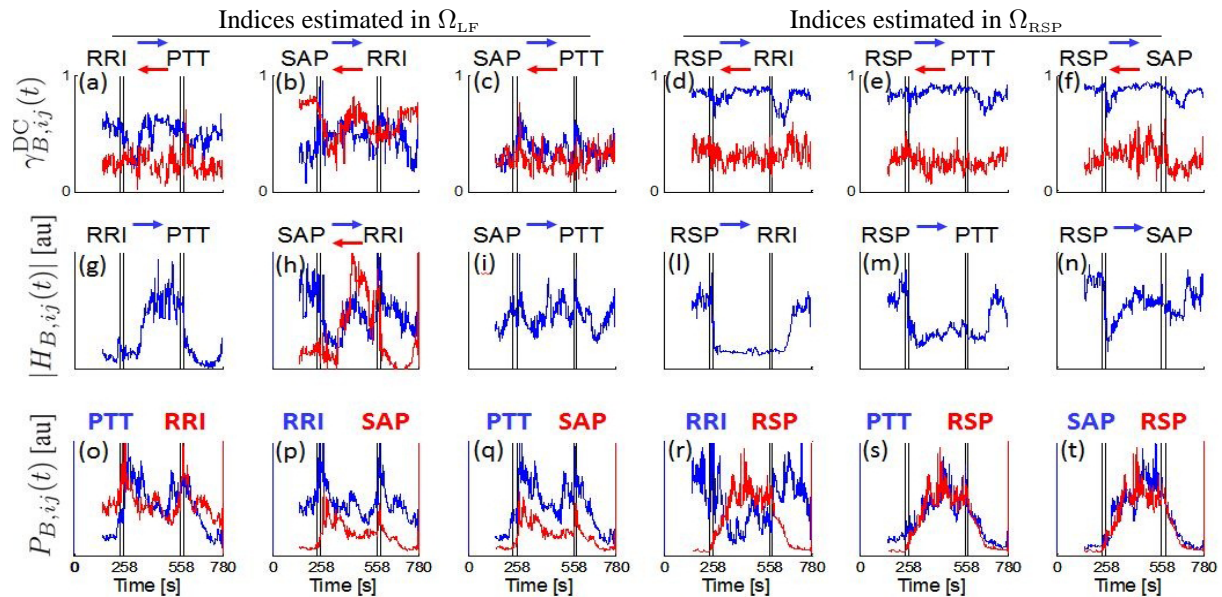


Figure 2. Median time course of the indices estimated across subjects. Upper graphics: directed coherence,  $\gamma_{ij}^{DC}(t)$ ; pathways  $j \rightarrow i$  and  $i \rightarrow j$  are plotted in blue and red, respectively. Graphics on the middle: gains of the transfer functions,  $|H_{ij}(t)|$ . Lower graphics: instantaneous powers,  $P_{ii}(t)$ . Gains and powers are in arbitrary units [au], for easier comparison (we are mainly interested in temporal changes). Vertical lines mark  $T_{ES}$ ,  $T_{HT}$  and  $T_{LS}$ .

autonomic-mediated baroreflex changes were faster than vasculature-mediated changes along the RRI→SAP direction.

Future works should include the exploration of additional variables, such as diastolic arterial pressure or central venous pressure, different model orders, the assessment of the latencies between coupled oscillations, and other indices of interaction, including statistical analyses to assess significant strength of the directional couplings.

## Acknowledgements

This work was supported in part by NIH grant R01-HL084502, and by Ministerio de Ciencia y Tecnología, FEDER under Project TEC2010-21703-C03-02, and TRA2009-0127, and by ARAID and Ibercaja under project Programa de apoyo a la I+D+i. First and second authors contributed equally to this work.

Address for correspondence:

Luca Citi, PhD, 55 Fruit Street, Jackson 4, Boston, MA 02114. email: lciti@neurostat.mit.edu

## References

[1] Saul JP, Berger RD, Albrecht P, Stein SP, Chen MH, Cohen RJ. Transfer function analysis of the circulation: unique insights into cardiovascular regulation. *Am J Physiol Heart Circ Physiol* 1991;261(4):H1231–H1245.  
 [2] Barbieri R, Bianchi A, Triedman J, Mainardi L, Cerutti S,

Saul J. Model dependency of multivariate autoregressive spectral analysis. *IEEE Eng Med Biol Mag* 1997;16:74–85.  
 [3] Aletti F, Bassani T, Lucini D, Pagani M, Baselli G. Multivariate decomposition of arterial blood pressure variability for the assessment of arterial control of circulation. *IEEE Trans Biomed Eng* 2009;56(7):1781–1790.  
 [4] Naschitz JE, Bezobchuk S, Mussafia-Priselac R, Sundick S, Dreyfuss D, Khorshidi I, Karidis A, Manor H, Nagar M, Peck ER, Peck S, Storch S, Rosner I, Gaitini L. Pulse transit time by R-wave-gated infrared photoplethysmography: review of the literature and personal experience. *J Clin Monit Comput* Dec 2004;18(5-6):333–342.  
 [5] Faes L, Nollo G. *Biomedical Engineering, Trends in Electronics, Communications and Software*. 2011; .  
 [6] Barbieri R, Matten EC, Alabi AA, Brown EN. A point-process model of human heartbeat intervals: new definitions of heart rate and heart rate variability. *American Journal of Physiology Heart and Circulatory Physiology* 2005; 288(1):H424–H435.  
 [7] Gil E, Orini M, Bailón R, Vergara JM, Mainardi L, Laguna P. Photoplethysmography pulse rate variability as a surrogate measurement of heart rate variability during non-stationary conditions. *Physiol Meas* 2010;31(9):1271.  
 [8] Mincholé A, Pueyo E, Rodríguez JF, Zacur E, Doblaré M, Laguna P. Quantification of restitution dispersion from the dynamic changes of the T-wave peak to end, measured at the surface ECG. *IEEE Trans Biomed Eng* May 2011; 58(5):1172–1182.  
 [9] Porta A, Bassani T, Bari V, Pinna G, Maestri R, Guzzetti S. Accounting for respiration is necessary to reliably infer granger causality from cardiovascular variability series. *IEEE Trans Biomed Eng* Dec 2011; .